Geomagnetic storms caused by shocks and ICMEs

Veronica Ontiveros[1] and J. Americo Gonzalez-Esparza[2]

Received 16 March 2010; revised 25 May 2010; accepted 24 June 2010; published 26 October 2010.

[1] We performed an event-by-event study of 47 geomagnetic storms (GSs) that occurred during the ascending phase of solar cycle 23. All the GSs are associated with the passage of a shock and an interplanetary coronal mass ejection (ICME). For each event, we identified the section in the interplanetary (IP) medium causing the GS (the sheath behind the shock, the main body of the ICME or the combination of both). On average, the most intense GSs are caused by sheaths, followed by sheath-ICME combinations and by ICMEs. We obtained the correlation coefficients between the intensity of each GS (minimum Dst) and several solar wind parameters. We found that the well-known correlation between the GS intensity and the solar wind convected electric field, E_y, stands for the GSs caused by ICMEs (CC = −0.88) and sheath-ICME combinations (CC = −0.95), but it is very low for the GSs caused by sheaths (CC = −0.44). In contrast, we found a very good correlation between the GSs caused by sheaths and the total convected electric field (ΣE_y) (CC = −0.89). On the other hand, we estimated the total perpendicular pressure (P_t) for each IP event associated with the GSs and identified the three different types of P_t profiles. The most intense GSs are related with IP events with $P_t = 1$, but moderate and less intense storms are associated with the three P_t profiles. The correlations between the Dst and the solar wind parameters results that the CCs decrease significantly for IP events having a P_t profile of 3.

Citation: Ontiveros, V., and J. A. Gonzalez-Esparza (2010), Geomagnetic storms caused by shocks and ICMEs, *J. Geophys. Res.*, *115*, A10244, doi:10.1029/2010JA015471.

1. Introduction

[2] Geomagnetic storms (GSs) are caused by solar wind structures impacting and injecting material into the magnetosphere. In general, moderate and intense GSs are mainly related with the passing interplanetary coronal mass ejections (ICMEs) driving shock waves [e.g., *Russell et al.*, 1974; *Echer and Gonzalez*, 2004; *Echer et al.*, 2008]. Based on in situ observations we identify three sections in the large-scale structure of a shock-ICME event associated with the origin of a GS: (1) the interplanetary (IP) shock wave, (2) the sheath region behind the shock, and (3) the main body of theICME. When the interplanetary magnetic field associated with the sheath or in the ICME is antiparallel respect to the Earth's magnetic field, there is a magnetic reconnection process that injects and accelerates particles into the inner magnetosphere resulting in a ring current enhancement. This current induces a magnetic field aligned in opposite direction of the Earth's magnetic field at equatorial and middle latitudes, causing a depression in its horizontal component, B_H, which is the main signature of a GS. The disturbance storm time index, Dst, measures the intensity of the GS and is a proxy of the energy injection into the ring current by the solar wind disturbance [*Gonzalez et al.*, 1994 and references therein].

[3] A typical GS associated with the passing of a shock and its ICME proceeds as follows: a *sudden storm commencement*, characterized by an abrupt Dst increment due to the compression of the magnetosphere by the shock wave hitting the Earth environment; the *main phase*, where Dst decreases due to the ring current enhancement; and finally the Dst *recovery phase* that can last up to several days. Figures 1, 2, and 3 show examples of GSs caused by shock-ICME events, where we can recognize the three shock-ICME sections and the three GS phases that we commented on before. From left to right, the first solid line set the shock passage in the solar wind and the sudden storm commencement in the Dst index. The dash lines show the start and final times for the passage of the ICME accordingly with *Cane and Richardson* [2003], and the dotted lines at the bottom panel show the GS main phase interval in the Dst index.

[4] Figure 1 shows the GS on 22 October 1999, an event analyzed in detail by *Dal Lago et al.* [2006]. It can be inferred from the plots that this GS was caused by the trailing part of the ICME, where the source of B_s is a fast stream following the ICME. *Dal Lago et al.* pointed out how this interaction leads to a very intense GS, despite the fact that the solar source of the ICME is an average-speed CME. Figure 2 shows an intense GS on 12 August 2000. This GS was caused by the sheath-ICME combination, where the low beta plasma parameter and the rotation of the B_z component

[1]Posgrado en Ciencias de la Tierra, Instituto de Geofisica, Universidad Nacional Autonoma de Mexico, Mexico City, Mexico.
[2]MEXART, Unidad Michoacan, Instituto de Geofisica, Universidad Nacional Autonoma de Mexico, Morelia, Mexico.

0148-0227/10/2010JA015471

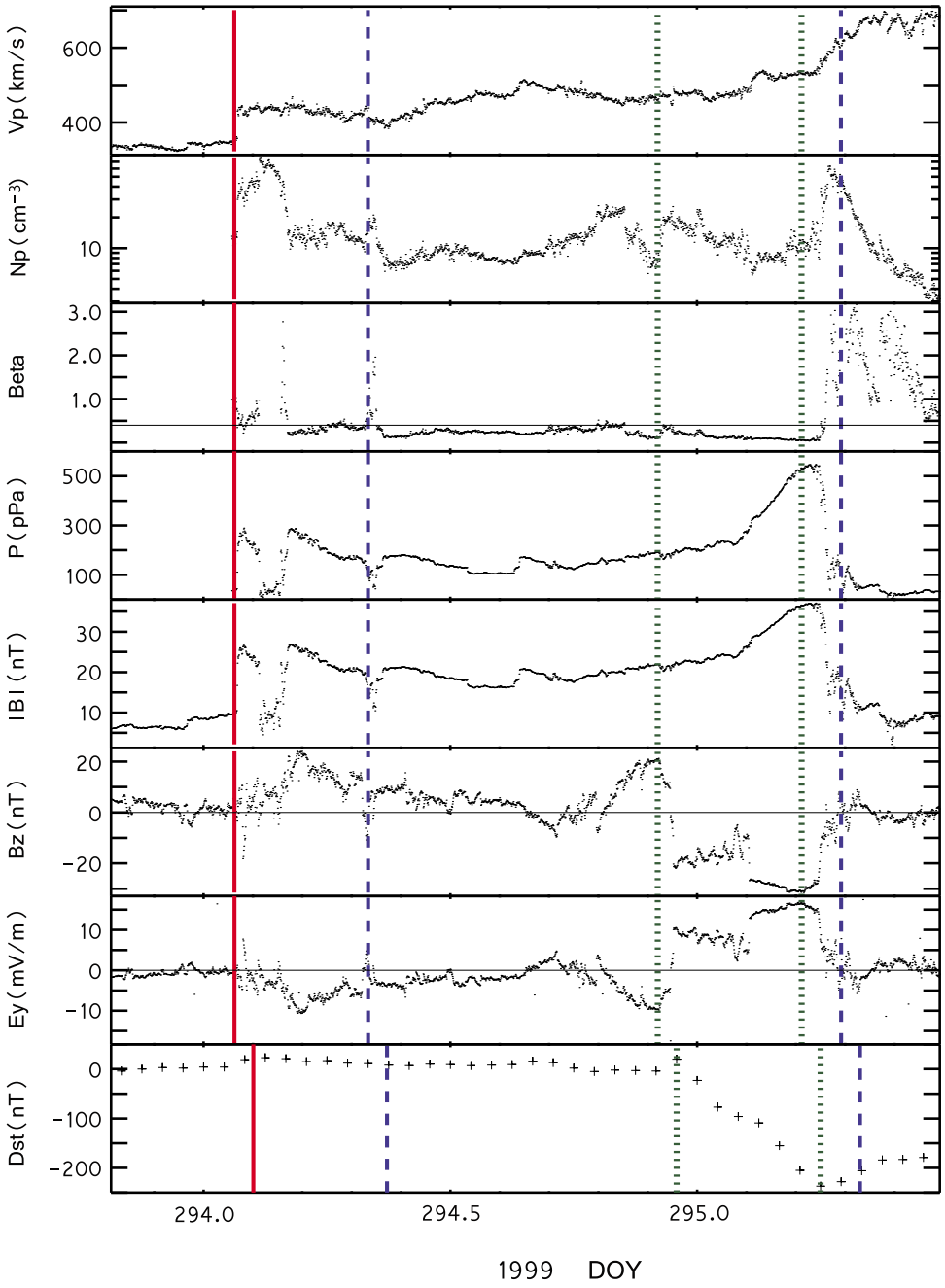

Figure 1. Geomagnetic storm on 22 October 1999. Plasma parameters at 1 AU observed by ACE compared with the Dst index. The solid line is the shock passage in the IP medium and the sudden storm commencement in the Dst. The dashed lines are the start and end of the ICME as reported by *Cane and Richardson* [2003]. The dotted lines denote the interval for the main phase of the GS. This is an example of a GS caused by an ICME, with the pressure profile in group 2.

indicate the passage of a magnetic cloud. Finally, Figure 3 shows an intense GS on 7 April 2000. This GS was caused by the sheath which has an important B_z south component just after the passage of the shock.

[5] There are several statistical studies of the geoeffectiveness of IP disturbances. *Echer et al.* [2008] concluded that magnetic clouds driving fast shocks are the most geoeffective events causing about 48% of the intense GS over the raising phase of solar cycle 23. *Huttunen et al.* [2002] analyzed 111 GSs for the same period, finding that 32% of its moderate storms are associated with the passage of an ICME and 50% of the intense ones are due to the combination of the sheath and ICME driving the shock. On the other hand, the minimum value reached by the Dst (regardless of the shock-ICME section causing the GS) is well correlated with two parameters: (1) the south component of the magnetic field, B_s, and (2) the electric field convected by the solar

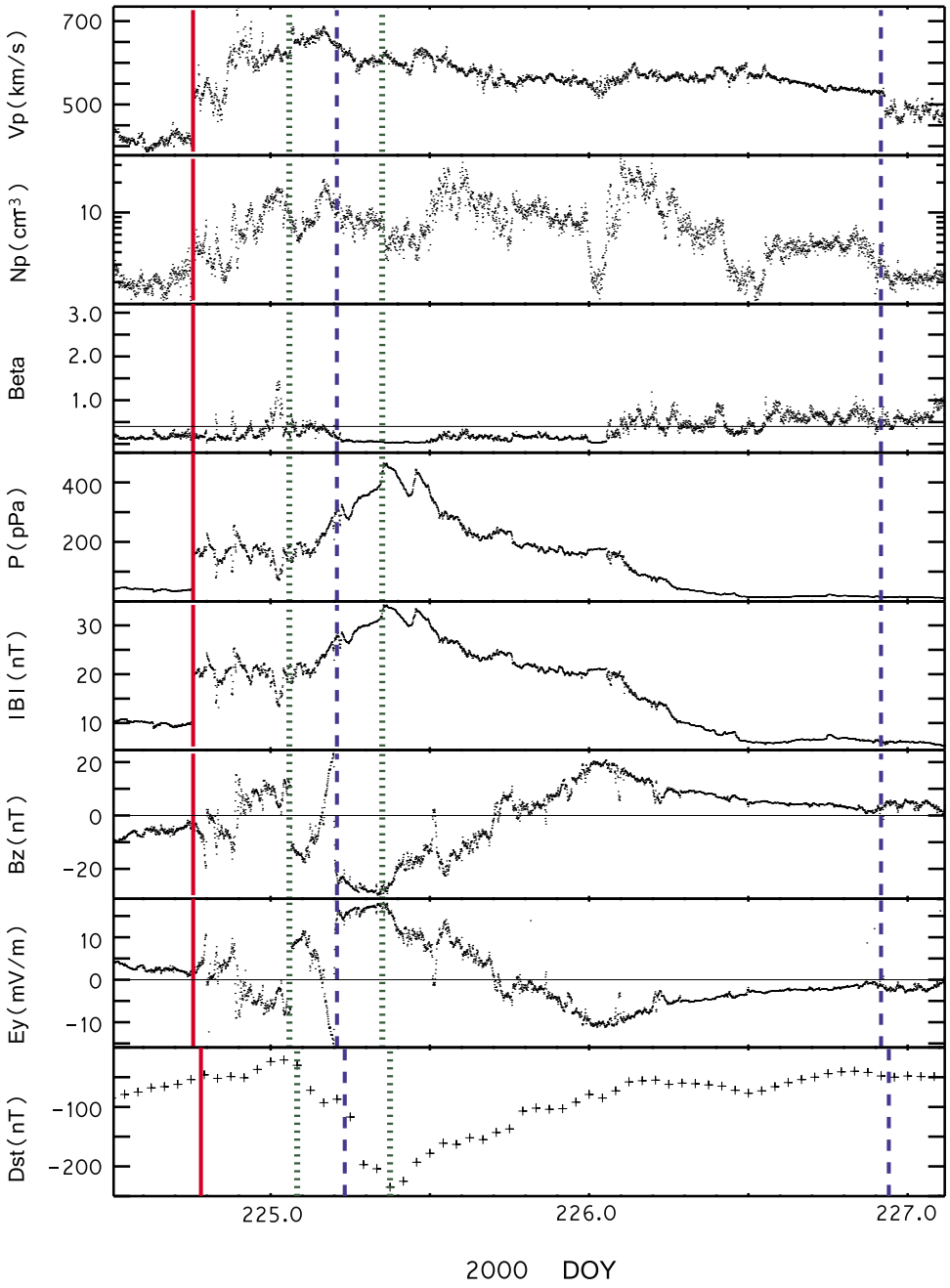

Figure 2. Geomagnetic storm on 12 August 2000. Plasma parameters at 1 AU observed by ACE compared with the Dst index. The solid line is the shock passage in the IP medium and the sudden storm commencement in the Dst. The dashed lines are the start andend of the ICME as reported by *Cane and Richardson* [2003]. The dotted lines denote the interval for the main phase of the GS. This is an example of a GS caused by the sheath-ICME, with pressure profile in group 1.

wind, $E_y = VB_s$, over the interaction time [e.g., *Russell et al.*, 1974; *Gonzalez and Tsurutani*, 1987].

[6] *Wang et al.* [2003] found for 105 GSs a correlation coefficient of 0.92 between the Dst and E_y and that a combination of values of $\langle Bs \rangle > 3$ nT and interaction time >1 h lead to moderate GSs (−50 nT > Dst > −100 nT), whereas a combination of values of $\langle Bs \rangle > 6$ nT and interaction time >3 lead to intense ones (Dst ≤ −100 nT). Similar values and correlations have been found by several authors [e.g., *Wu and Lepping*, 2002; *Echer et al.*, 2008]. In the case of the energy injection rate, *Vieira et al.* [2004] analyzed 20 intense GSs finding that the GSs caused by sheath fields evolves faster than the ones caused by the main body of the ICME. This result suggests a different response of the magnetosphere regarding of the energy injection rate (E_y/interaction time).

[7] The total perpendicular pressure ($P_t = B^2/(2\mu_o) + \sum_j n_j k T_{\mathrm{perp},j}$, where j represents proton, electron, and α

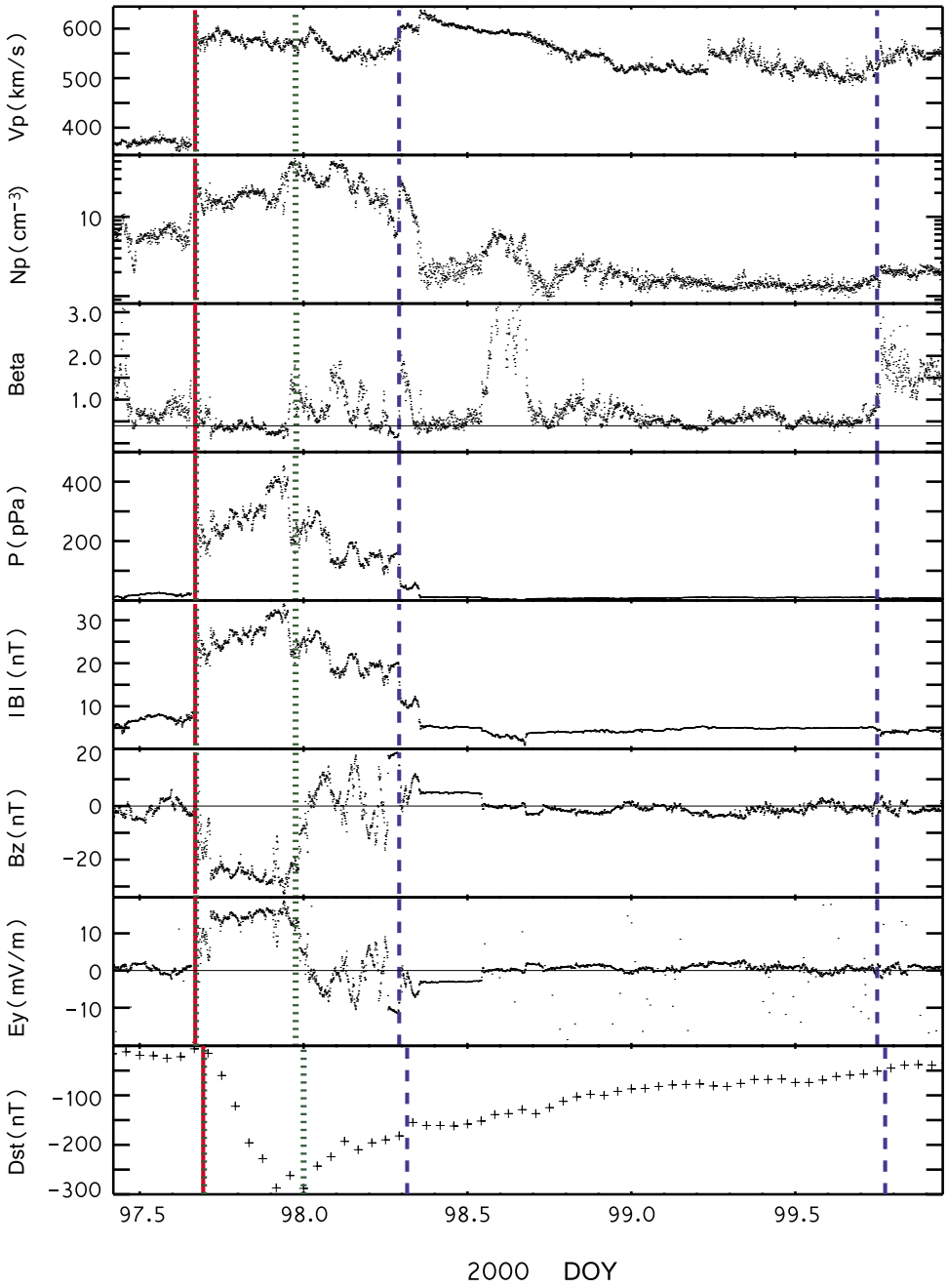

Figure 3. Geomagnetic storm on 7 April 2000. Plasma parameters at 1 AU observed by ACE compared with the Dst index. The solid line is the shock passage in the IP medium and the sudden storm commencement in the Dst. The dashed lines are the start and end of the ICME as reported by *Cane and Richardson* [2003]. The dotted lines denote the interval for the main phase of the GS. This is an example of a GS caused by the sheath, with pressure profile in group 3.

particles) can be used to identify the passing of a shock-ICME through the Earth's environment and could give us an approximation of the shock-ICME crossing line by the spacecraft [*Russell et al.*, 2005]. The P_t profiles can be organized in three groups which may indicate the crossing around the shock-ICME nose, offset from the shock-ICME central part, or through the flank of the shock [*Jian et al.*, 2006]. Therefore it is interesting to investigate the relationship between the P_t profiles of the shock-ICME events and their geoeffectiveness.

[8] The aim of this paper is to perform a case-by-case study of GSs produced by shocks and ICMEs to analyze how the sections of the shock-ICME event are related with the minimum Dst and how these are related with their P_t profiles.

2. Event Selection and Methodology

[9] In order to select single GSs caused by only one shock-ICME event, we used the Dst final values from the

Table 1. The 47 GSs[a]

ev	Year	Month	Day	H	min Dst	IP cause	Pressure Profile
1	1998	Jun	14	10	−55	Sh-ICME	1
2	1998	Jun	26	4	−101	Sh-ICME	1
3	1998	Aug	20	20	−67	ICME	1
4	1998	Aug	27	9	−155	ICME	2
5	1998	Sep	25	9	−207	Sh-ICME	1
6	1998	Oct	19	15	−112	Sh-ICME	1
7	1998	Nov	9	17	−142	ICME	1
8	1999	Jan	13	23	−112	ICME	1
9	1999	Feb	18	9	−123	Sheath	2
10	1999	Mar	10	8	−81	Sheath	2
11	1999	Apr	17	7	−91	ICME	1
12	1999	Sep	22	23	−173	ICME	3
13	1999	Oct	22	6	−237	ICME	2
14	1999	Dec	13	9	−85	ICME	1
15	2000	Feb	12	11	−133	Sheath	1
16	2000	Apr	7	0	−288	Sheath	1
17	2000	Jun	8	19	−90	Sh-ICME	2
18	2000	Jul	20	9	−93	ICME	3
19	2000	Jul	29	11	−71	ICME	3
20	2000	Aug	12	9	−235	Sh-ICME	1
21	2000	Oct	4	20	−143	ICME	1
22	2000	Oct	5	13	−182	Sheath	3
23	2000	Oct	14	14	−107	ICME	1
24	2000	Oct	29	3	−127	ICME	3
25	2000	Nov	6	21	−159	Sheath	1
26	2000	Nov	27	1	−80	Sheath	3
27	2000	Nov	29	13	−119	ICME	2
28	2001	Jan	24	18	−61	ICME	3
29	2001	Mar	5	2	−73	ICME	2
30	2001	Mar	20	13	−149	Sh-ICME	1
31	2001	Apr	9	6	−62	Sheath	3
32	2001	Apr	11	23	−271	Sheath	1
33	2001	Apr	13	15	−77	ICME	2
34	2001	Apr	18	6	−114	Sheath	3
35	2001	Apr	22	15	−102	ICME	1
36	2001	Aug	17	21	−105	Sheath	3
37	2001	Oct	1	8	−148	Sheath	3
38	2001	Oct	12	12	−71	Sheath	1
39	2001	Oct	21	21	−187	Sheath	3
40	2001	Oct	28	11	−157	Sheath	3
41	2001	Dec	30	5	−58	ICME	1
42	2002	Mar	1	1	−71	ICME	1
43	2002	Mar	24	9	−100	Sh-ICME	1
44	2002	Apr	18	7	−127	Sheath	2
45	2002	May	23	17	−109	Sheath	3
46	2002	Aug	1	13	−51	ICME	1
47	2002	Aug	2	5	−102	Sheath	2

[a]The date and hour reported are for the time of min D_{st}.

World Data Center for Geomagnetism, the list of ICMEs identified by *Cane and Richardson* [2003], and the list of IP shocks detected by ACE [*http://www-ssg.sr.unh.edu/mag/ace/ACElists/obslist.html*]. From the D_{st} database, we identified 110 moderate GSs and 51 intense GSs occurred from June 1998 to August 2002. From these 161 events we choose all those which satisfied our criteria selectionto know that (1) the geomagnetic storm has a sudden storm commencement undoubtedly associated with an IP shock passage as observed by ACE spacecraft; (2) the IP shock is part of a shock-ICME system, where the ICME is reported by *Cane and Richardson* [2003]; and (3) there are available plasma and magnetic field parameters (observed by ACE) before, during, and after the shock-ICME system passage.

[10] Trying to set a one-to-one association between the GSs and the shock-ICME system, we discarded those cases where we found more than one GSs associated with the same shock-ICME and with a significant Dst recovery in between (e.g., a GS caused by the sheath and a second one caused by the trailing part of the ICME). Finally, we discarded those GSs where the Dst in the main phase did not reach a lower value than the one previous to the IP shock arrival. Under these considerations, the final set of events in our study consists of 47 GSs (17 moderate and 30 intense).

[11] For each event we identified the section of the shock-ICME event associated with the main phase of the GS. The main phase starts where the Dst decreases to lower values than the ones previous to the sudden storm commencement and it ends where the Dst reaches its minimum value. The duration of the main phase defines the interaction time.

[12] In order to correlate the in situ spacecraft measurements and the magnetic ground observations we need to take into account the *delay time* that relates both observations. *Gonzalez and Echer* [2005] proposed a 2 h delay time according to their study on correlating the peak of maximum B_s in the solar wind and the minimum Dst. However, the delay time varies on a case-by-case basis according to the position of the spacecraft and the speed of the solar wind perturbation. In this case-by-case study we define the delay time as the interval between the IP shock passage at the spacecraft and the sudden storm commencement measured by the Dst. The delay time differs for each GSand can go from 20 min up to 1 h. The interval between the two solid lines in Figures 1–3 (the passing of the shock and the sudden storm commencement at the ground) defines the delay time between the two observations. Using this delay time we shifted the interaction time to the solar wind data from the shock passage. The dotted lines in Figures 1–3 show the interaction time in the solar wind data and the GS main phase interval in the Dst. Once the data are shifted and plotted together, we can recognize the geoeffective section in the IP structure. The geoeffectiveness of the shock-ICME system could come either from the sheath section, the ICME section, or a combination of both. Figure 1 shows a GS caused by the trailing part of the ICME, Figure 2 shows a GS caused by the combination sheath-ICME, and Figure 3 shows a GS caused by the sheath.

[13] We also analyzed the P_t profile of all the shock-ICME events and classified them as group 1, 2, or 3 following the *Russell et al.* [2005] description. In group 1, P_t increases rapidly at the sheath and piles up to a central maximum in the later magnetic obstacle. According with *Russell et al.* this group would correspond a crossing close to the nose of the shock-ICME. In group 2, P_t presents a rapid rise at the sheath, a pressure plateau, and, much later, a return to earlier lower pressure values. This group would correspond to a crossing offset from the nose that results in a flat pressure profile in the center that can be followed by a decrease or increase at the trailing part. In group 3, P_t presents a monotonic decrease of the pressure profile and would correspond to a crossing at the flank of the shock. In principle, according with the former interpretation, since all our events have ICME signatures following the shock, we would expect very few P_t group 3 events in our study. The three P_t profiles are shown in Figures 1–3: Figure 1 is a group 2, Figure 2 is a group 1 P_t, and Figure 3 is a group 3 example where the value decreases fast after the shock passage and gets minimal values inside the ICME.

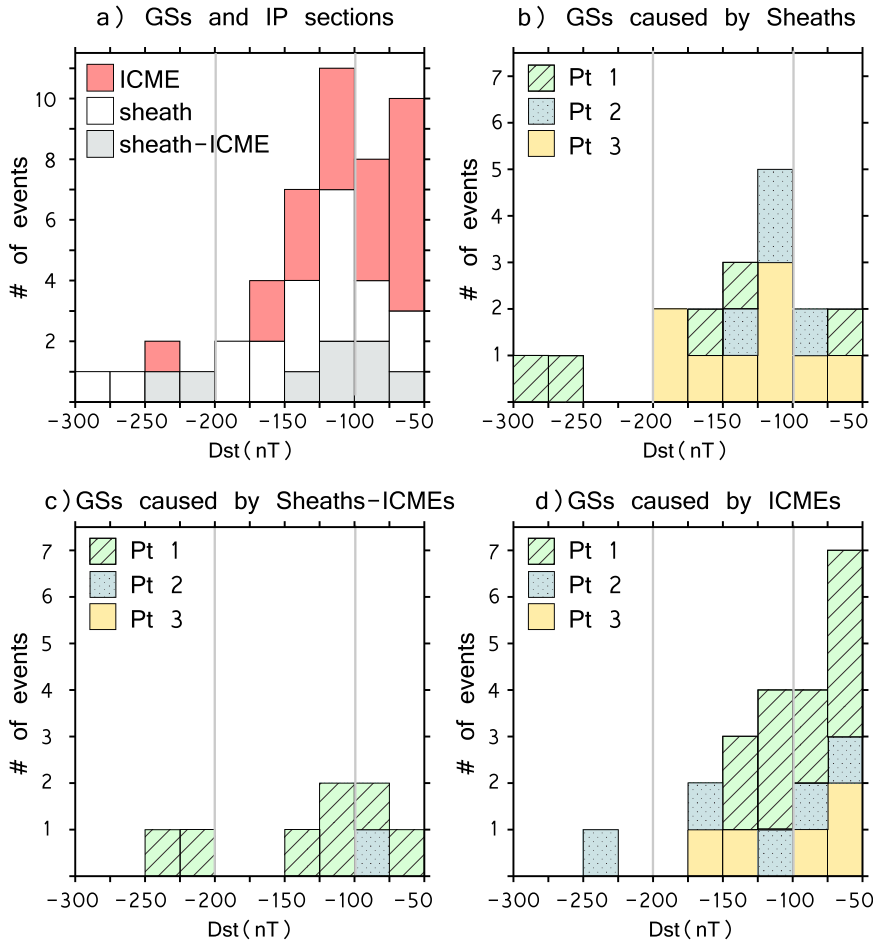

Figure 4. Distribution frequency of the intensity of the GSs and their IP causes. (a) all the events, (b) GSs caused by sheaths, (c) GSs caused by sheath-ICME combinations, and (d) GSs caused by ICMEs. Figures 4a–4c show the distributions of their P_t profiles.

[14] The final set of 47 events consist of 17 moderate and 30 intense GSs. Table 1 shows the final list for this study. Column 1 is the number of event, columns 2 to 5 are the date and hour of the minimum Dst for each GS, column 6 is the cause of the GS in the IP medium (sheath, ICME, or the combination of both), and column 7 is the corresponding group for the P_t profile.

3. Results and Discussion

[15] The 30 intense GSs we selected are almost 60% of the original sample (51 events). Having more than one half of the total intense events, we assume that our set is representative of the intense GSs. To reinforce this point, we run a simple Kosmogorov-Smirnov test, a statistical method for comparing two samples, that works fine both in small and large amount of events [*James*, 2006, and references therein]. Comparing the *goodness of fit* between the Dst distribution for the original 51 intense GS with the Dst distribution of the 30 GSs in our study, we obtained that the maximum difference between the cumulative distributions is $D = 0.0588$. This low value is telling us that there is a very high confidence of our selected events are indeed representative of the total intense GSs observed.

[16] On the other hand, the 17 moderate storms in or set are just a few percentages (15%) of the total observed (110 events). This selection might not be representative of all the moderate GS, but this was expected since it is common that moderate GS are caused by other IP structures [e.g., *Russell et al.*, 1974; *Echer and Gonzalez*, 2004].

[17] Figure 4 presents histograms showing the relationship between the Dst minimum and the IP sections causing the GSs. The number of GSs caused by ICMEs (44.6%) is comparable with the ones caused by sheaths (38.3%), whereas the GSs caused by the combination of both is a minor fraction (17%). Figure 4a shows that there is no trend in moderate or intense GSs but they seem to be caused by the three IP sections. The average of the Dst minima of the GSs caused by sheaths is -139 ± 62 nT; that of the GSs caused by sheath-ICME combinations is -131 ± 61 nT; and that of the GSs caused by ICMEs is -105 ± 45 nT. However, the five most intense GSs in the study (Dst < 200 nT) were caused by the three IP sections. In Figures 4b, 4c, and 4d we separate the GSs by their IP causes indicating the distribution of their P_t profiles. Figure 4c shows that seven of the eight GSs caused by combinations sheath-ICME have $P_t = 1$.

[18] From the solar wind parameters observed in situ by ACE, we obtained average and maximum values of the

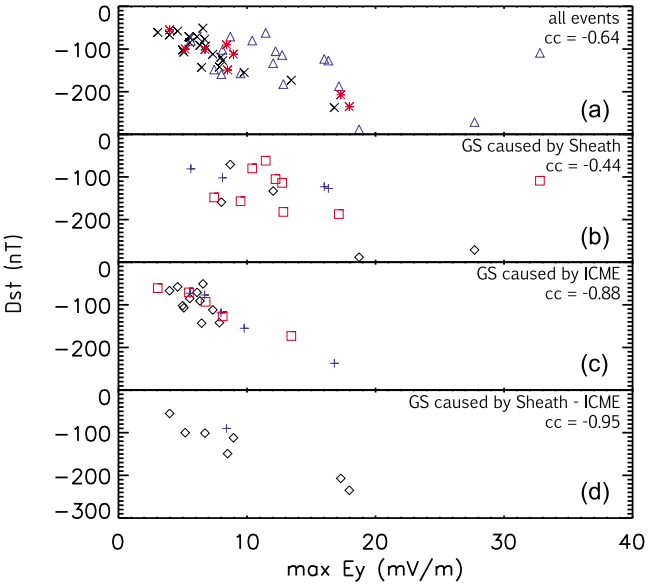

Figure 5. Dispersion plot for max E_y versus Dst. (a) All events, (b) GSs caused by sheath, (c) GS caused by ICME, and (d) GS caused by sheath-ICME.

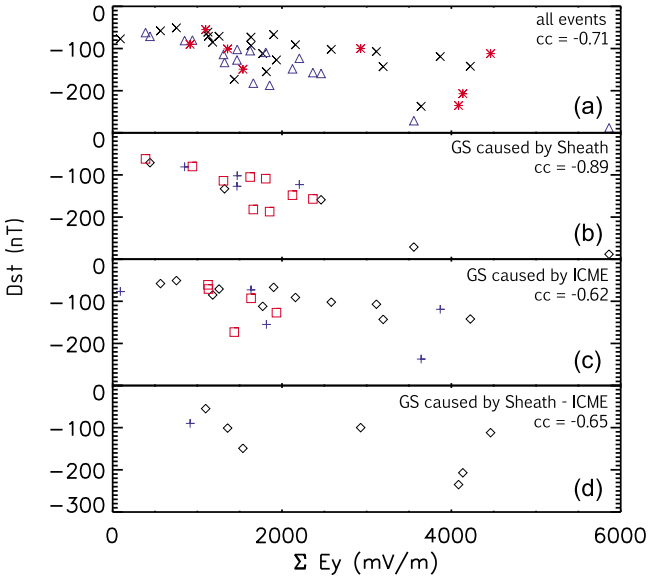

Figure 6. Dispersion plot for ΣE_y versus Dst. (a) All events, (b) GSs caused by sheath, (c) GS caused by ICME, and (d) GS caused by sheath-ICME.

south component of the IP magnetic field, B_s, and the convected electric field, $E_y = VB_s$, during the interaction time. Figure 5 shows the dispersion plot for Dst versus the maximum of E_y, which is probably the most well-known correlation. From top to bottom, the first panel shows all the GSs where the symbol code is as follows: (Δ) GSs caused by sheaths, (×) caused by ICMEs, and (*) caused by sheath-ICME combinations. We do not find a high correlation coefficient (CC) between the Dst and max E_y (CC = −0.64). This result is lower than that in previous studies, for example, the one obtained by *Wu and Lepping* [2002] (CC = 0.79), where their study was restricted to a set of 35 geoeffective magnetic clouds occurred between 1995 and 1998. However, the results of CCs modify when the IP section causing the GS is taken in account. Figures 5b, 5c, and 5d separate the 47 GSs by its IP cause: sheath, ICME, or sheath-ICME combinations (the symbol code refers to their P_t profiles: (◇) $Pt = 1$, (+) $P_t = 2$, and (square) $P_t = 3$). In this case, the GSs caused byICMEs or sheath-ICME combinations present high correlations (CC = −0.88 and CC = −0.95 respectively), which in fact are higher than the result by *Wu and Lepping*.

[19] The result that called our attention is the low correlation between the Dst and max E_y for the GSs caused by sheaths (CC = −0.44). Wondering about this, we tried correlations with different parameters, in particular, ΣE_y, which is defined as the sum of E_y through the interaction time. We considered only the E_y positive values since this component is partly responsible for the ring current injection [e.g., *Russell et al.*, 1974; *Burton et al.*, 1975; *Gonzalez and Tsurutani*, 1987]. In addition, after an eye inspection of the plots, we are confident that the E_y negative values do not last long enough for a significant recovery of the Dst during the main phase of each storm.

[20] Figure 6 shows the dispersion plots for Dst versus ΣE_y, in the same format as that in Figure 5. We find a very good correlation (CC = −89) for the GSs caused by sheaths (second panel). In contrast, there are lower correlations for the GSs caused by sheath-ICMEs (CC = −0.62) and for those caused by ICMEs (CC = −0.65).

[21] These results suggest to us that the magnetosphere responds differently to sheaths as compared to ICMEs and the differences in the CCs for GS caused by sheaths is a consequence of this phenomena. It is certainly a very interesting finding although the different responses should perhaps be expected given that the sheaths have different properties than the ICMEs components (e.g., higher turbulence and higher dynamic pressure). We plan to pursue this further in a future paper.

[22] Table 2 summarizes the correlation coefficients (CCs) between the Dst and several parameters in the shock-ICME events. Column 1 indicates the CCs of Dst with respect to the maximum and average values of B_s and E_y during the interaction time and with respect to ΣE_y/interaction time, which is a proxy of the rate of energy injected to the interior of the magnetosphere by the total convected electric field over the interaction time. Columns 2 to 4 show the CCs when the GSs are separated in their IP causes. The GSs caused by ICMEs and sheath-ICME combinations show very similar results of CCs for the different parameters,

Table 2. Correlation Coefficients Between the Min Dst and Several Parameters in the Solar Wind, and the Values for the Three Sections Causing the GSs

		Caused by		
Dst vs.	All Events	Sheath	ICME	Sh-ICME
max B_s	−0.68	−0.50	−0.81	−0.89
$\langle Bs \rangle$	−0.61	−0.35	−0.76	−0.70
max E_y	−0.64	−0.44	−0.88	−0.95
$\langle E_y \rangle$	−0.66	−0.30	−0.88	−0.93
ΣE_y	−0.71	−0.89	−0.62	−0.65
ΣE_y/int time	−0.75	−0.54	−0.85	−0.91

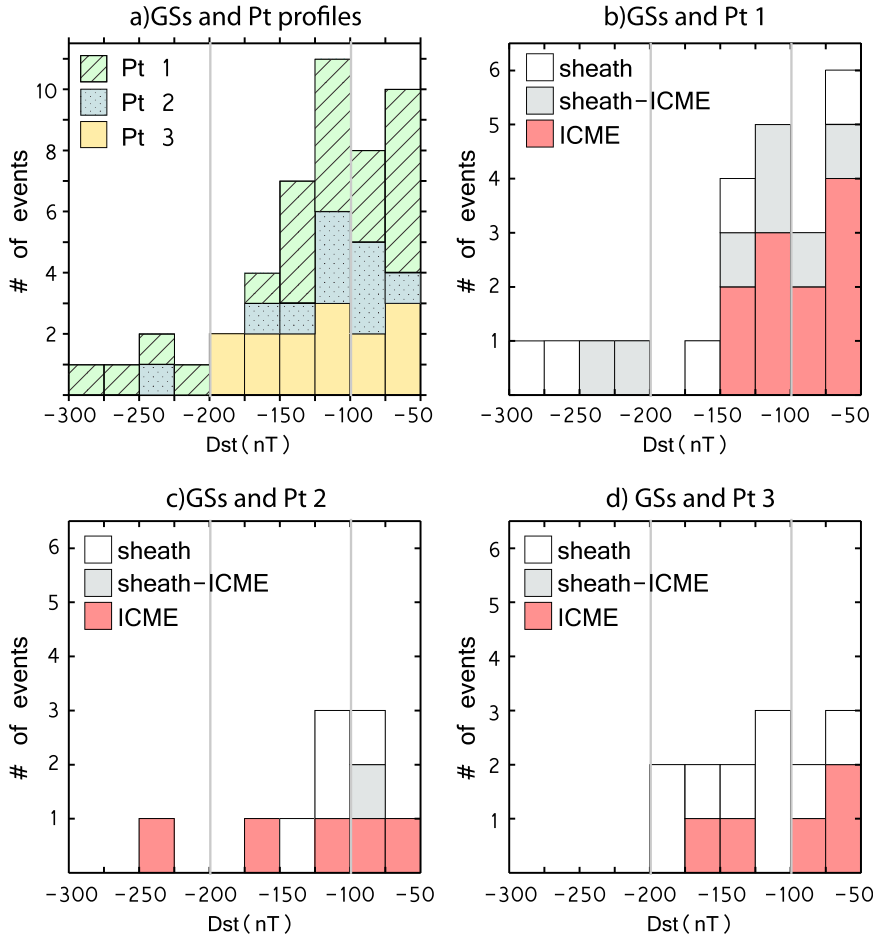

Figure 7. Distribution frequency of the intensity of the GSs and their P_t profiles. (a) All events, (b) GSs caused by $P_t = 1$, (c) GSs caused by $P_t = 2$, and (d) GSs caused by $P_t = 3$. The last three panels show the distributions of the cause of their IP.

where the highest correlations are for the maximum and average of the B_s and E_y components. This result is expected since the very existence of the south component of the magnetic field is a requirement for the magnetic reconnection, and the convected electric field increases the ring current. What is interesting is that the GSs caused by sheaths (the most intense GSs subset in our study) show a different behavior and, as commented above in Figures 5 and 6, these GSs only present a good CC with ΣE_y. This variation of the CCs suggest different responses of the magnetosphere depending on the IP event causing the GS. The accumulated convected electric field ΣE_y is a better parameter for the GSs caused by sheaths.

[23] Figure 7 presents a series of histograms to study the relationship between the Dst minimum and the P_t profiles associated with the GSs. The relevance of this relationship lies on the fact that the P_t profile does not depend on the interaction time and can be measured in situ independently from the GS. Figure 7a shows that about half (48.9%) of the GSs were associated with shock-ICME events having a $P_t = 1$, which could mean that, in these cases, the magnetosphere was impacted by the nose region of the shock-ICME event. The average of the Dst minima related with these GSs with $P_t = 1$ is -126 ± 67 nT. The 21.3% of the GSs have $P_t = 2$ and their average of the Dst minima is -118 ± 49 nT; and the 29.8% of the GSs have $P_t = 3$ and the average of their Dst minima is -119 ± 44 nT. For those moderate and intense GSs with a minimum Dst > −200 nT, we do not find any clear trend between the P_t profiles and the GS intensities; however, four of the five superstorms in the study (Dst ≤ −200 nT) have $P_t = 1$. It has to be considered that the pressure profile groups distribution might be biased by the criteria of the event selection, therefore the pressure profile analysis is complementary, but it is not conclusive. However, this result could favor looking for the most intense GSs among those caused by IP structures with $P_t = 1$ profile.

[24] In Figures 7b, 7c, and 7d we separate the GSs by their P_t profiles and therefore show the distribution of their IP causes. Figure 7b shows the distribution of GSs with $P_t = 1$. We find the three IP causes for moderate and intense GSs with Dst > −150 nT, but in the case of the four most intense ones (Dst < −200 nT) they were caused by sheaths (two events) or combination of sheaths-ICMEs only (two events). This result agrees with previous studies where it has been found that the compressed sheath field leads to intense GSs [e.g., *Tsurutani et al.*, 1992; *Jurac et al.*, 2002], as well as fast ejectas (in particular magnetic clouds) driving shocks [e.g., *Echer et al.*, 2008].

Table 3. Correlation Coefficients Between the Min Dst and Several Parameters in the Solar Wind, and the Values for the Total Perpendicular Pressure Profiles of the Shocks-ICMEs

	Pressure Profile Groups		
Dst vs.	1	2	3
max B_s	−0.87	−0.69	−0.43
$\langle Bs \rangle$	−0.63	−0.83	−0.62
max E_y	−0.89	−0.73	−0.26
$\langle E_y \rangle$	−0.80	−0.90	−0.42
ΣE_y	−0.77	−0.69	−0.68
ΣE_y/int time	−0.75	−0.86	−0.79

[25] Figure 7c shows the distribution of GSs with $P_t = 2$. In this case there is only one GS (of 10) caused by a combination sheath-ICME. Figure 7d shows the GSs with $P_t = 3$. All the GSs with $P_t = 3$ have Dst minima > −200 nT, and there are no GSs caused by the sheath-ICME combination.

[26] In general, since all the events have ICME signatures, we would expect this group to be small in the data set, but it is about one third of the events. This result is not contradictory since we do not use the total pressure profiles to identify the passage of the ICMEs, and it is used only to approach the line of crossing of the ICME. We believe that the origin of this disagreement relies on the high dependence the ICME detection has on the solar wind parameters considered.

[27] Table 3 reports the CCs of the GSs separated in the three groups of pressure profiles P_t. The GSs with $P_t = 1$ have good (higher than 0.8) CCs with max B_s, max E_y, and $\langle E_y \rangle$, whereas the GSs with $P_t = 2$ have goodCCs with max $\langle B_s \rangle$, $\langle E_y \rangle$, and ΣE_y/interaction time. All these CCs are comparable with the ones found when considering the ICME or shock-ICME as the cause the GS. On the other hand, the GSs with $P_t = 3$ show lower CCs than the ones for $P_t = 1$ and $P_t = 2$ for four of the six considered IP parameters.

4. Summary and Conclusions

[28] We studied a set of 47 GSs associated with the passage of an ICME and its driven shock. We calculated different correlations between the intensity of the GSs with plasma, magnetic, and electric field parameters. The correlation coefficients vary taking into account the three sections causing the main phase of the GS: (1) the sheath behind the shock, (2) the main body of the ICME, or (3) the combination of both.

[29] GSs caused by ICMEs or sheath-ICME combinations are well correlated with the maximum and average value of the magnetic field south component B_s and the convected electric field E_y estimated over the interaction time. However, GSs causedby sheaths show low correlations with the same parameters, but they have good correlation with the accumulated field, ΣE_y, during the interaction time.

[30] We used the total perpendicular pressure P_t profile criteria of *Russell et al.* [2005] to study its relationship with the GS intensities. This profile can be used to approximate the line crossing of the spacecraft through the ICME. In general, the most intense GSs are related with IP events having $P_t = 1$. Those IP events with $P_t = 1,2$ tend to increase the correlations coefficients between the Dst index and the solar wind parameters, whereas the IP events with $P_t = 3$ tend to decrease the same correlations. This suggest that the crossing of the IP structure through its nose or its flank affects the way that the magnetosphere responses to the IP structures.

[31] **Acknowledgments.** V. Ontiveros thanks CONACyT for her Ph.D. grant. J.A. Gonzalez-Esparza is grateful for the financial support by the CONACyT 48494 and PAPIIT IN105310 projects.

[32] Philippa Browning thanks Jeff Morrill and another reviewer for their assistance in evaluating this manuscript.

References

Burton, R. K., R. L. McPherron, and C. T. Russell (1975), An empirical relationship between interplanetary conditions and Dst, *J. Geophys. Res.*, *80*, 4204–4214, doi:10.1029/JA080i031p04204.

Cane, H. V., and I. G Richardson (2003), Interplanetary coronal mass ejections in the near-Earth solar wind during 1996–2002, *J. Geophys. Res.*, *108*(A4), 1156, doi:10.1029/2002JA009817.

Dal Lago, A., et al. (2006), The 17–22 October (1999) solar-interplanetary-geomagnetic event: Very intense geomagnetic storm associated with a pressure balance between interplanetary coronal mass ejection and a high-speed stream, *J. Geophys. Res.*, *111*, A07S14, doi:10.1029/2005JA011394.

Echer, E., and W. D. Gonzalez (2004), Geoeffectiveness of interplanetary shocks, magnetic clouds, sector boundary crossings and their combined occurrence, *Geophys. Res. Lett.*, *31*, L09808, doi:10.1029/2003GL019199.

Echer, E., W. D. Gonzalez, B. T. Tsurutani, and A. L. C. Gonzalez (2008), Interplanetary conditions causing intense geomagnetic storms (Dst = −100 nT) during solar cycle 23 (1996–2006), *J. Geophys. Res.*, *113*, A05221, doi:10.1029/2007JA012744.

Gonzalez, W. D., J. A. Joselyn, Y. Kamide, H. W. Kroehl, G. Rostoker, B. T. Tsurutani, and V. M. Vasyliunas (1994), What is a geomagnetic storm?, *J. Geophys. Res.*, *99*(A4), 5771–5792.

Gonzalez, W. D., and B. T. Tsurutani (1987), Criteria of interplanetary parameters causing intense magnetic storms (Dst of less than −100 nT), *Planet. Space Sci.*, *35*, 1101–1109.

Gonzalez, W. D., and E. Echer (2005), A study on the peak Dst and peak negative Bz relationship during intense geomagnetic storms, *Geophys. Res. Lett.*, *32*, L18103, doi:10.1029/2005GL023486.

Huttunen, K. E. J., H. E. J. Koskinen, and R. Schwenn (2002), Variability of magnetospheric storms driven by different solar wind perturbations, *J. Geophys. Res.*, *107*(A7), 1121, doi:10.1029/2001JA900171.

James, F. (2006), *Statistical Methods in Experimental Physics*, 2nd ed., World Scientific, Singapore.

Jian, L., C. T. Russell, J. G. Luhmann, and R. M. Skoug (2006), Properties of interplanetary coronal mass ejections at one AU during 1995 2004, *Solar Phys.*, *239*, 393–436.

Jurac, S., J. C. Kasper, J. D. Richardson, and A. J. Lazarus (2002), Geomagnetic disturbances and their relationship to interplanetary shock parameters, *Geophys. Res. Lett.*, *29*(10), 1463, doi:10.1029/2001GL014034.

Russell, C. T., R. L. McPherron, and R. K. Burton (1974), On the cause of geomagnetic storms, *J. Geophys. Res.*, *79*(7), 1105–1109.

Russell, C. T., A. A. Shinde, and L. Jian (2005), A new parameter to define interplanetary coronal mass ejections, *Adv. Space Res.*, *35*, 2178–2184.

Tsurutani, B. T., Y. T. Lee, W. D. Gonzalez, and F. Tang (1992), Great magnetic storms, *Geophys. Res. Lett.*, *19*(1), 73–76.

Vieira, L. E. A., W. D. Gonzalez, E. Echer, and B. T. Tsurutani (2004), Storm-intensity criteria for several classes of the driving interplanetary structures, *Solar Phys.*, *223*, 245–258.

Wang, Y., C. L. Shen, S. Wang, and P. Z. Ye (2003), An empirical formula relating the geomagnetic storm's intensity to the interplanetary parameters: −VBz and delta *t*, *Geophys. Res. Lett.*, *30*(20), 2039, doi:10.1029/2003GL017901.

Wu, C.-C., and R. P. Lepping (2002), Effects of magnetic clouds on the occurrence of geomagnetic storms: The first 4 years of Wind, *J. Geophys. Res.*, *107*(A10), 1314, doi:10.1029/2001JA000161.

J. A. Gonzalez-Esparza, MEXART, Unidad Michoacan, Instituto de Geofisica, Universidad Nacional Autonoma de Mexico, Tzintzuntzan 310, Vista Bella, 58098 Morelia, Michoacan, Mexico.

V. Ontiveros, Posgrado en Ciencias de la Tierra, Instituto de Geofísica, Universidad Nacional Autonoma de Mexico, Ciudad Universitaria, Coyoacan, 04510 Mexico City, Mexico. (ontiveros@geofisica.unam.mx)